Q^2 for HAPPEX-2

Tim Holmstrom
College of William and Mary

Robert Feuerbach, Robert Michaels
Thomas Jefferson National Accelerator Facility

(Dated: March 7, 2005)

In this report we discuss the measurements of Q^2 for the HAPPEX-Helium and HAPPEX-Hydrogen runs in 2004 summarized in Table I.

I. ENERGY AND MOMENTUM

The four-momentum transfer squared is

$$Q^2 \;=\; 2\,E\,E'\,(1-\cos(\theta)) \tag{1}$$

where E is the incident energy, E' is the final momentum or energy of the electron ($E' \gg m_e$) and θ is the scattering angle. For the elastic peak one may eliminate one of the three variables, which provides a consistency check.

For the beam energy we used the ARC measurement in halog 129163.

$$E \;=\; 3.0258 \;\pm\; 0.00032 \text{ (stat)} \;\pm\; 0.0006 \text{ (syst)} \;\; \text{GeV} \tag{2}$$

I.e. the errors are 0.32 and 0.6 MeV statistical and systematic. For both helium and hydrogen, we assumed a 3 MeV average energy loss to the center of the target and applied this as a correction to the energy. Although the error in eq. 2 is very small, we assumed an error of 3 MeV in our error budget, which is a conservative error based on the history of discrepancies among energy measurements and drifts in the accelerator setup.

The error in the momentum E' was assumed to be 5 MeV. This is consistent with the observed shifts in the missing mass, see figure 9. We did *not* correct for these shifts.

II. CENTRAL SCATTERING ANGLE

The largest systematic error contribution is from the scattering angle. This is because we are at very forward angle. This section reports on a new method to determine this angle with better accuracy than can be achieved from surveying. The method, suggested by Nilanga Liyanage, relies on measuring the energy of elastically-scattered electrons off of different nuclei to determine the angle of the spectrometers. The measured energy (E') of the scattered electron is related to the incident beam energy (E_0), scattering angle (θ) and mass of the initial (m) and recoiling nucleus (m^*) through:

TABLE I: Q^2 **for 2004 HAPPEX Runs**

	Helium Run	Hydrogen Run
L-arm Q^2 $(\text{GeV})^2$	0.0939 ± 0.0009 (1 %)	0.1018 ± 0.001 (1 %)
R-arm Q^2 $(\text{GeV})^2$	0.0892 ± 0.0009 (1 %)	0.0957 ± 0.001 (1 %)

$$E' + \varepsilon' = \frac{E_0 - \varepsilon_0 - \frac{1}{2m}(m^{*2} - m^2)}{1 + (1 - \cos\theta)(E_0 - \varepsilon_0)/m} \tag{3}$$

where ε_0 and ε' are the energy loss of the incident and detected electrons. In practice, $\varepsilon' = \varepsilon_0$ and are each assigned half the energy loss due to ionization in the target. The scattered electrons from only the central sieve hole (D4) were compared for multiple targets and momentum settings.

A. Targets

Energy loss due to ionization was calculated using the Bethe-Block equation. The target specifications are given in Table II as well as the expected energy loss from ionization. The beam-line and spectrometer were under vacuum, so only energy-loss at the target is considered. The total energy loss due to ionization was equally divided between the incident beam (ε_0) and the final state electron (ε').

Target	Material	Density (mg/cm^2)	Ionization dE (MeV)
Single Carbon foil	^{12}C	200	0.66
Water cell	0.001 inch Steel window	20	0.06
	5mm H_2O	500	1.87
	0.001 inch Steel window	20	0.06
	Total:	540	1.99

TABLE II: The target parameters and energy loss for the 2004 HAPPEX-II run. The energy loss was calculated assuming a 3 GeV beam.

B. Energy Distribution

The energy loss due to bremmstrahlung was accounted for in the shape of the electron energy spectrum peaks. The peak-shape was chosen as a gaussian convoluted with an exponential, with the analytic result given as:

$$f(x) = \sqrt{\frac{\pi}{2}}\frac{\sigma}{\alpha}\exp\left[\frac{1}{2\alpha}(\sigma^2/\alpha + 2*(b-x))\right]\mathrm{Erfc}\left(\frac{|\alpha|}{\sqrt{2}\sigma\alpha}(\sigma^2/\alpha + (b-x))\right) \tag{4}$$

where α describes the exponential fall-off $e^{(b-x)/\alpha}$ when $(\alpha x > b)$, σ is the width of the Gaussian, b is the peak of the un-smeared distribution, and x is the reconstructed energy of the scattered electron $x = P_0(1+\delta+\triangle\delta)$. Here P_0 is the central momentum setting of the spectrometer; δ is the fraction difference of the reconstructed momentum from P_0; and $\triangle\delta$ is the second-order correction to δ that was found to be necessary, locally taking into account imperfections in the reconstruction matrix. The function $\mathrm{Erfc}(z)$ is the complementary error function, $\mathrm{Erfc}(z) \equiv 1 - \mathrm{Erf}(z) = \frac{2}{\sqrt{\pi}}\int_z^\infty e^{-t^2}dt$.

The reliability of the reconstructed δ and momentum was checked by comparing the scattered electron spectra off the carbon and water targets for different momentum settings of the spectrometer. The stepping between momentum settings were chosen as to have the elastic and excited-state peaks from the oxygen and carbon overlap with the elastic hydrogen peak at an adjacent setting, as shown in Figure 1. The relations between the NMR readback and the central momentum of the spectrometers were taken from JLAB-TN-01-049 (2001) (N. Liyanage).

The carbon and water-cell spectra were fit for the central hole for each kinematic setting, with Eqn 4 describing the shape of each peak, with all peaks in a spetrum sharing common values of α and P_0. The "true" location of each peak b is calculated directly from the Equation 3 using the known values of E_0, m, and m^{*2}, and trial values of θ.

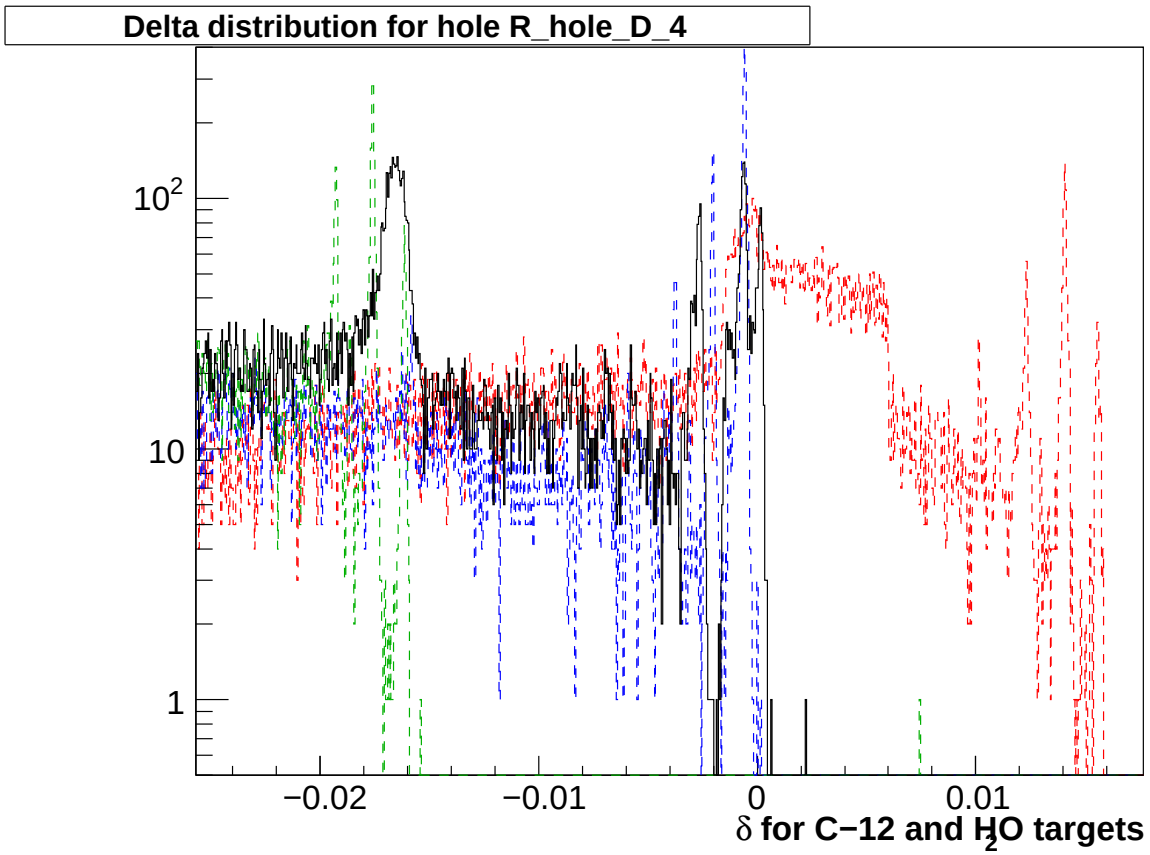

FIG. 1: The δ distribution seen by the R-HRS off the carbon (colored dashed-lines) and water (black solid-line) targets for different spectrometer momentum settings. The central momentum settings for the R-HRS were 2.9846, 3.0328, and 3.0811 GeV/c for the red, blue and black, and green curves, respectively.

Parameters	Value (MeV)
E_0	3025. $\triangle\theta = 0.002°$/MeV
$m(^1H)$	938.27
$m(^{16}O)$	14895.08
$m(^{16}O_{3m}) - m(^{16}O)$	6.13
$m(^{16}O_{2p1m}) - m(^{16}O)$	7.12
$m(^{12}C)$	11174.86
$m(^{12}C_{2p}) - m(^{12}C)$	4.44
$m(^{12}C_{0p}) - m(^{12}C)$	7.65
$m(^{12}C_{3m}) - m(^{12}C)$	9.64
$m(^{56}Fe)$	52089.78
$m(^{56}Fe_{2p}) - m(^{56}Fe)$	4.32

TABLE III: The parameters fixed parameters used in the fit of the E' distributions. The beam energy E_0 was varied slightly, in the fits, and a weak dependence was observed. For the runs used, the beam energy was held and observed to be constant.

The list of fixed parameters used in the fit are given in Table III. The read-back beam energy during these runs was constant, so we believe the beam energy was fixed to better than 3 MeV, which is in our error budget.

The sieve holes saw a finite range of angles, as shown in Figure 2, and for the hydrogen target this effect had to be taken into account. This "dp-kin" effect is referred to as the *kinematic correction* in this document. The effect on the extracted angle of this kinematic correction was a systematic shift of the scattering angles of 0.015°. Since the correction was expected to not have a large effect on the angular reconstruction (the average δ for each hole would

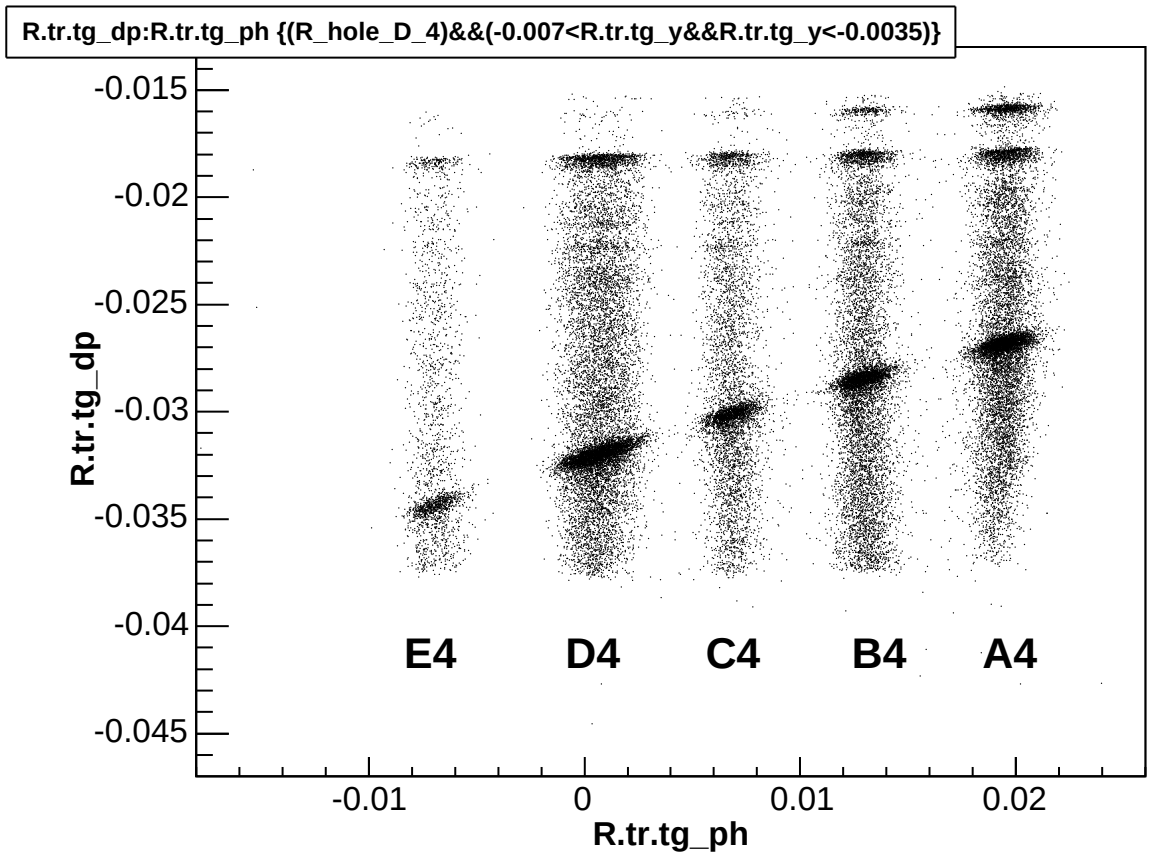

FIG. 2: The dependence of δ on the in-plane angle,ϕ, dependence, for the central row of sieve holes. This correlation was removed with the *kinematic correction*.

stay the same) the final result contains entries from analysis both before and after the correction.

C. Central Angle Results

A sample fit can be seen in Figure 3 for the R-HRS. For the L-HRS, the presence of multiple-trigger sources underneath the peaks of the heavier nuclei (O and Fe) for the moderate momentum settings, and beneath the H peak for the low momentum setting, led to fits of lesser quality. To compensate, the offset $\triangle\delta$ was determined from the carbon-foil runs and tested against fits with the hydrogen alone. Also, the highest-momentum setting run (1072) was used in the angular determination since, even though the momentum calibration could not be checked, the peak shapes were not distorted. The results from all the fits are presented in Table IV.

The overall average angles seen by the R-HRS and L-HRS spectrometers, taking into account all the different variations, were found to be $5.94 \pm 0.02°$ and $6.13 \pm 0.02°$, respectively. These may be compared to the survey results which were $5.87 \pm 0.05°$ and $6.05 \pm 0.05°$ (note the larger error for the surveys). The location of the water cell was found to be centered 0.6mm downstream of the nominal target center, causing a shift of $+0.004°$, well less than the systematic uncertainty.

The uncertainty was driven primarily by the unexpected variation of the extracted angle after the kinematic corrections were applied.

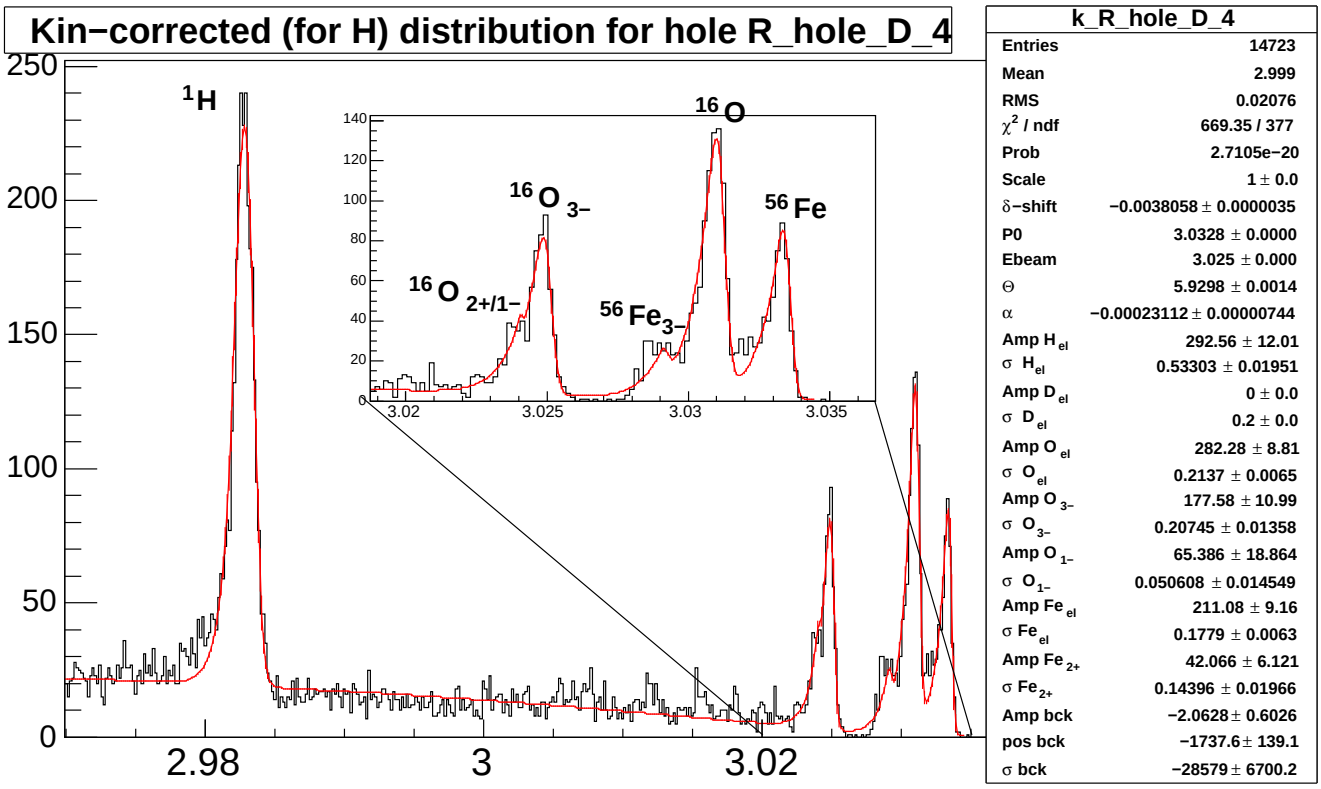

FIG. 3: A fit to the central hole of the R-HRS sieve, from run 1080, after kinematic corrections

III. SPECTROMETER MATRIX ELEMENTS

The purpose of the optics database is to allow the determination of particle momentum and the target variables y, θ, and ϕ from the focal plane variables x, y, θ and ϕ. These databases are well established and tested for the standard HRS running in Hall A but the addition of the new septum magnets created the need for a new database.

The first septum experiment to run in Hall A was Small Angle GDH. That experiment used only the right Septum and HRS, with the Left HRS being used in standard mode. The experiment ran at many different momentum settings, which required a new database for the right arm. However, this database, which was obtained by Vince Sulkosky, was not useful for HAPPEX, with its two septa, because the septum fringe fields affect each other. During the Hypernuclear experiment, which used both septa and ran just prior to HAPPEX, a new database was obtained by Yi Qiang for the Left and Right HRS+Septum, but this did not use an extended target, nor was it for our momentum. Thus a new optics database optimization was needed for HAPPEX.

To accomplish this optimization special optics runs were taken at the start of the experiment. Three targets were used: a single foil C12 target, a two foil C12 target with 12 cm spacing, and a two foil C12 target with 24 cm spacing. The data was taken at a series of four different momentums. All data was taken with the standard 7x7 Hall A Sieve slits. These slits are designed so that the center hole and orientation of the holes can be determined even with a poor database.

The code used for the optimization was C++ code developed by Nilanga Liyanage which was ported to the "Podd" analyzer by Ole Hansen and Yi Qiang. The optimization code uses a TRANSPORT tensor to link the variables x, y, θ, and ϕ of the focal plane to the variables delta momentum, θ, ϕ, and y of the target. The x position at the target is assumed to be equal to the x beam position. The tensors can be up to fifth order polynomials of the focal plane variables. The optimization code then varies some tensors of one target variable to match the sieve pattern to the locations determined by the geometry of the sieve and the foils. A χ^2 minimization technique with MINUIT is

TABLE IV: **Recoil Angle Determination Parameters**

R-HRS					
Run	Target	p_0 (GeV/c)	$\triangle\delta(10^{-3})$	$\Theta_0(^\circ)$	Comment
1068	^{12}C foil	3.0812	-3.742 (4)	5.944 (fixed)	
1073	^{12}C foil	3.0328	-3.724 (3)	5.944 (fixed)	
1092	^{12}C foil	2.9846	-3.778 (7)	5.944 (fixed)	
With kinematic corrections					
1080	H_2O	3.0382	-3.806 (4)	5.930 (2)	
		3.0271(1)	-7.470 (3)	5.941 (2)	
		3.0382	-3.724 (to 1073)	5.937 (2)	
		3.0382	-3.742 (to 1068)	5.921 (2)	(H-only)
		3.0382	-3.742 (to 1068)	5.935 (2)	
1097		2.9846	-3.902 (8)	5.926 (2)	
Without kinematic corrections					
1080	H_2O	3.0382	-3.795 (5)	5.944 (3)	
		3.0452(1)	-7.828 (6)	5.955 (3)	
		3.0382	-3.724 (to 1073)	5.952 (3)	
		3.0382	-3.742 (to 1068)	5.950 (3)	
1097		2.9846	-3.890 (9)	5.941 (4)	
Average				5.94 ± 0.02	

L-HRS					
Run	Target	p_0 (GeV/c)	$\triangle\delta(10^{-3})$	$\Theta_0(^\circ)$	Comment
1068	^{12}C foil	3.0791	-2.401 (5)	6.0 (fixed)	
1073	^{12}C foil	3.0308	-2.373 (3)	6.0 (fixed)	$\frac{d\triangle\delta}{d\theta} = -0.504 \cdot 10^{-3}$
1092	^{12}C foil	2.9825	-2.519 (8)	6.0 (fixed)	
With kinematic corrections					
1080	H_2O	3.0308	-2.600 (7)	6.143 (2)	
		3.0062(2)	-10.790 (58)	6.169 (2)	
		3.0308	-2.467 (to 1068)	6.124 (1)	(H-only)
		3.0308	-2.439 (to 1073)	6.119 (1)	(H-only)
1072		3.0791	-2.572 (8)	6.149 (2)	
Without kinematic corrections					
1080	H_2O	3.0308	-2.603 (7)	6.130 (4)	
		3.0308	-2.439 (to 1073)	6.106 (6)	poor ^{16}O fits
		3.0308	-2.467 (to 1068)	6.112 (6)	poor ^{16}O fits
1072		3.0791	-2.589 (9)	6.150 (4)	
Average				6.13 ± 0.02	

used by the program to determine the best tensor values. Since the target variables are related an iterative approach of optimizing one variable and then re-optimizing the other variables was used. For the HAPPEX optimization only the y target, ϕ target, and θ target were optimized. The δ momentum was not optimized since the lack of a uniform trigger made distinguishing the peaks difficult. The Momentum optimization of the Hypernuclear Experiment database should be acceptable for HAPPEX. The new S0 trigger will allow us to do this optimization for the 2005 run if we desire.

The optimized left and right θ versus ϕ sieve patterns are shown in Fig. 4. The line crossings show the calculated location for the sieve pattern. For both plots the center theta row is pushed toward the beamline. All septum optimizations have so far have seen this "kink". John LeRose believes that this is due to a separation of the Septum coils on the beam line side, which is difficult to model with the standard polynomials. This effect is worse in the Left Arm database. Vince has shown that this effect can be reduced but not removed by adding absolute value terms to the optimization tensor. This approach was not used for HAPPEX, but a preliminary study for our Left Arm data does show improvement. If this correction were deemed necessary, it could be implemented after some work. The θ versus ϕ sieve pattern for the left arm data from the $+6$ cm and -6 cm foils are shown in Fig. 5. The database gives similar results for all four momentum settings. The $+12$ cm and -12 cm foil data was not used in the main optimization.

We estimated the systematic error in Q^2 arising from matrix elements as follows. For the database calibrated by a

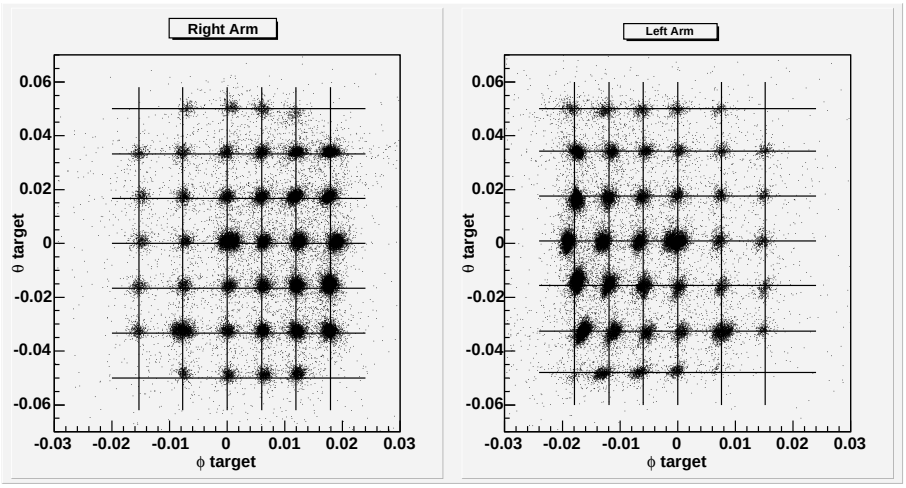

FIG. 4: The left plot shows the θ vs. ϕ sieve pattern for the right HRS+Septum system. The right plot shows the θ vs. ϕ sieve pattern for the left HRS+Septum system. The lines cross at the proper sieve positions.

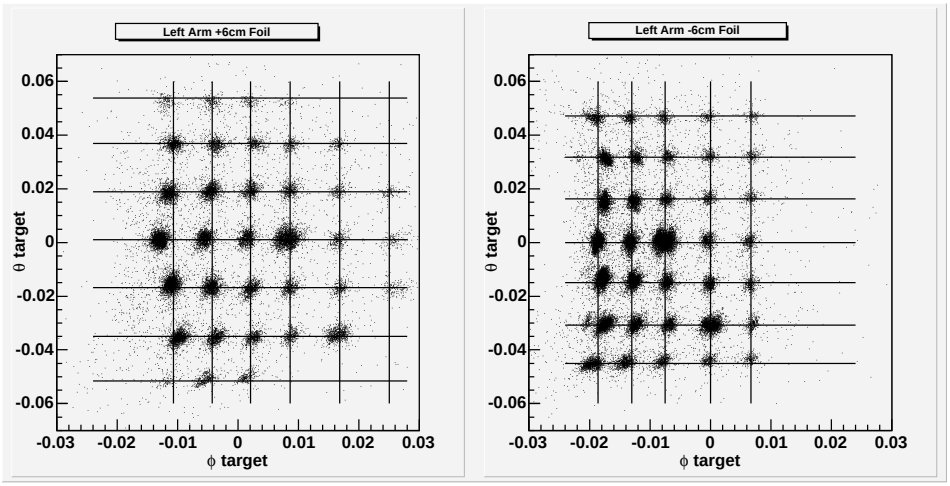

FIG. 5: The left plot shows the θ vs. ϕ sieve pattern for the left HRS+Septum system coming from the +6 cm foil. The right plot shows the θ vs. ϕ sieve pattern for the left HRS+Septum system coming from the -6 cm foil. The lines cross at the proper sieve positions.

target at $Z \approx 0$ (nominal target center), the position of each sieve hole was fit separately to find residuals errors in the angles. The average residuals on the Left HRS were 0.081 ± 0.58 mrad and 0.66 ± 1.4 mrad for the horizontal and vertical angles, respectively, where the sign convention is such that a positive residual occurs when the fitted value is larger than the matrix element value. Note, the horizontal angle is approximately the scattering angle, and the vertical enters Q^2 quadratically. For the Right HRS the residuals were 0.017 ± 0.41 mrad (horizontal) and 0.89 ± 1.1 mrad (vertical). The next step was to apply these corrections to the angles and observe the shift in Q^2. The algorithm used a grid of corrections with smooth interpolations in between grid points. Using these corrections we saw a shift in Q^2 of 0.1%. We decided to *not* apply this correction, and assigned a systematic error of 0.1% due to matrix elements from the $Z = 0$ database.

Next, to evaluate the Z dependence of the matrix element error, we used a database that was optimized with target foils at extreme locations, $Z = \pm 12$ cm and observed a shift in Q^2 of 0.5%. Although the average shifts from an extended target should be smaller, we took this 0.5% as a conservative estimate of the systematic error due to the Z dependence of matrix elements. It is listed along with the other errors in Table VI.

To summarize this subsection, the standard Hall A database optimization has been performed for ϕ target, θ target, and y target for the HAPPEX experiment. The database gives good results at four momentum settings for the center foil, +6 cm foil, and -6 cm foil. The systematic error at $Z = 0$ has been estimated by computing residuals in the

angles and observing the effect this has on Q^2. The error arising from the Z extent of the target has been estimated by using a database optimized on foils at ± 12 cm and observing the shift in Q^2. In 2005, the introduction of a new sweeper magnet will require us to calibrate the effect of this magnet. We plan to do this by making sieve measurements with the magnet on and off. In addition, the new S0 detector will provide cleaner triggers.

IV. ADC WEIGHTING

Since the integrating DAQ weights by energy, we need to do the same for the counting mode measurement of Q^2 by using the formula

$$Q^2 \;=\; \frac{(\Sigma\, Q_i^2\, W_i)}{(\Sigma\, W_i)} \tag{5}$$

where W_i is a weight factor for event i and Q_i^2 is the corresponding measurement. For the helium run, the W_i were simply the detector ADC values minus their pedestal. For the hydrogen run with two detectors it was necessary to adjust for their relative gains. Let $g2$ be the gain of the second detector relative to the first. Then we have $W_i = (g2 \times \mathrm{ADC}_1 - \mathrm{ADC}_2)_i$ where ADC_k is the ADC value minus pedestal for detector k. For helium, this weighting shifted Q^2 by -0.1%. For hydrogen the shift was different for L-arm and R-arm. For the L-arm the shift was $+0.28 \pm 0.10\%$ and for the R-arm it was $-0.45 \pm 0.1\%$ where the $\pm 0.1\%$ is the observed fluctuation from run to run. We'll take this fluctuation as the systematic error. We did not do the weighting separately for the two hydrogen detectors.

A negative sign of the shift is expected for the elastic peak, where $Q^2 \;=\; 2\, m_p\, (E - E')$. Here, the weighting enhances E' while the other variables are constant. On the other hand, an attenuation across the detector may either enhance or reduce the shift, depending on the orientation of the PMT relative to the high momentum direction. For helium the PMTs were on the high momentum end, and the attenuation was measured to be $\sim 0.4\%$ per cm on each spectrometer.

V. MISC. ERRORS

The drifts in time could be evaluated by using the UMass Q^2 scanner data, but this hasn't been done yet. Drifts in the accelerator energy have already been incorporated to some extent into the generous 3 MeV beam energy error. The experience with surveys indicate a good mechanical stability. However, during the hydrogen running, the Q^2 was measured near the beginning and end of the running period and was found to change by -0.1 % and $+0.4$ % for the Left and Right HRS respectively. For the R-HRS especially this change was much larger than the statistical uncertainty. Motivated by this observation, we assign a $\pm$ 0.2 % systematic in Q^2 from drifts.

The pileup effects can be estimated by comparing Q^2 for different cuts on the number of tracks in the event. Using a 1-track cut versus allowing multiple tracks makes a shift of -0.23 ± 0.1 % average shift on Q^2. We will take the variation in this as a systematic error.

VI. SUMMARY

Figure 6 shows the Q^2 distribution for the helium run, and figure 7 is for the hydrogen run. Figure 8 shows the Q^2 for the two hydrogen detectors separately. Keep in mind that the values in Table I have been ADC-weighted and are slightly different from the averages in the plots. Also, the hydrogen results are an average of five runs and the plots show only one run, while for helium there was only one Q^2 run.

TABLE V: **Summary of Errors in Q^2**

Error Source	Error (in source units)	Percent Error in Q^2
Scattering Angle	0.02 degrees	0.7 %
HRS Momentum Scale	5 MeV	0.2 %
Beam Energy	3 MeV	0.1 %
Matrix Elements:		
At Z = 0		0.1 %
Z dependence		0.5 %
ADC Weighting		0.1 %
Drifts in Time		0.2 %
Pileup		0.1 %
Total Systematic Error		1.0 %
Statistical Error		$\leq$0.1 %
TOTAL ERROR		1.0 %

We applied the following cuts :

1. The trigger must be defined by the detector(s). Using the scintillator trigger leads to a $\sim$ 0.1% shift.
2. The detector had a nonzero amplitude (ADC cut). For Hydrogen it did not matter if we cut on the sum of the two detectors or on the "or" of them.
3. There is only one track in the event.
4. The track must point back to within the acceptance at the target. Events that fail this cut introduce spurious tails in Q^2.

In table VI we summarize the errors which add in quadrature to 1.0 % error. The largest error contribution is from the scattering angle.

The improvements for the 2005 run are: a) Frequent scanner runs to check for drifts; b) The S0 detector will provide a cleaner trigger for the the sieve slit calibration and central angle recoil measurement.

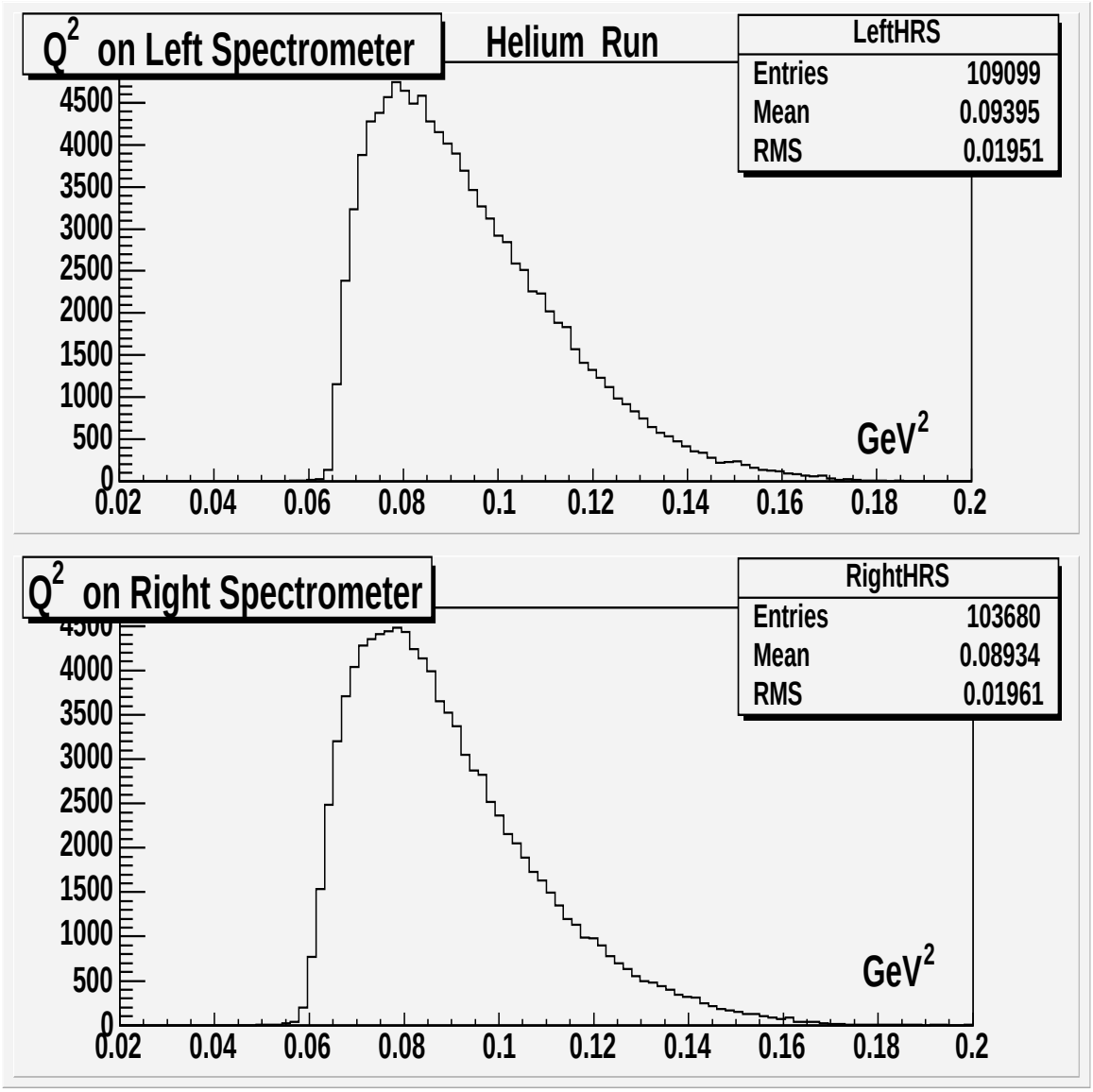

FIG. 6: Q^2 distribution for the 2004 HAPPEX Helium run

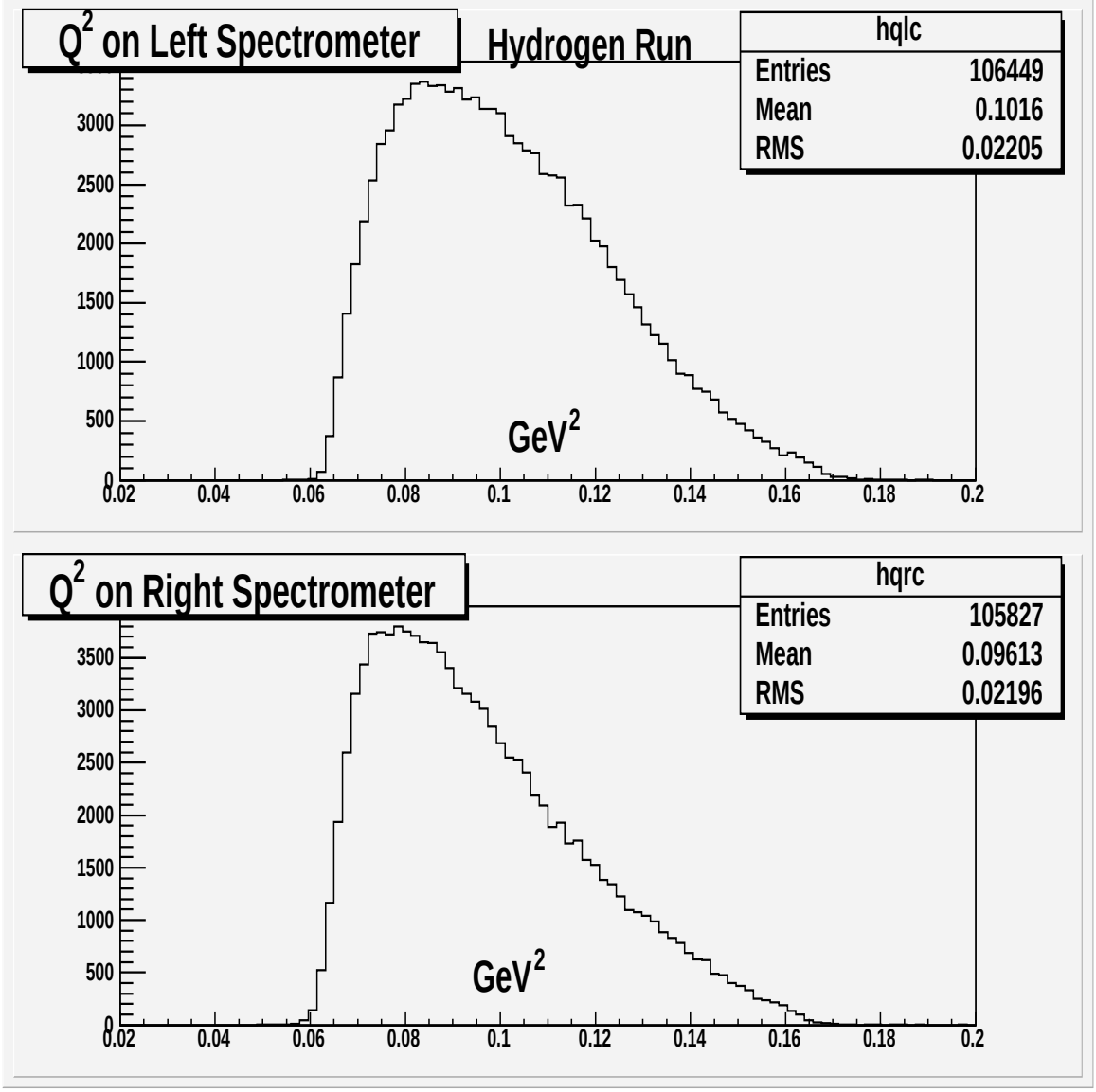

FIG. 7: Q^2 distribution for the 2004 HAPPEX Hydrogen run

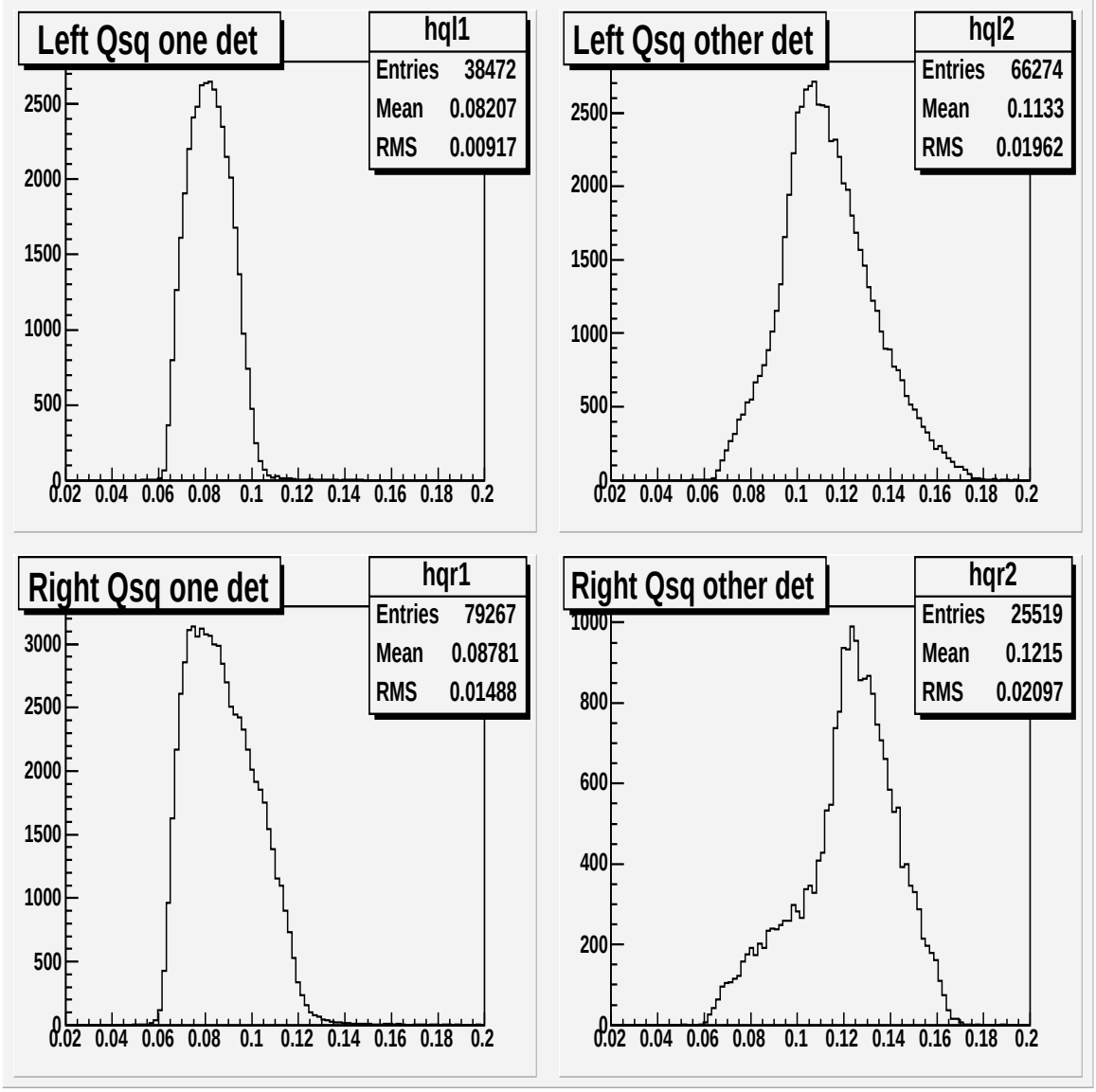

FIG. 8: Q^2 distribution for the 2004 HAPPEX Hydrogen run broken up into the two detector segments on each spectrometer.

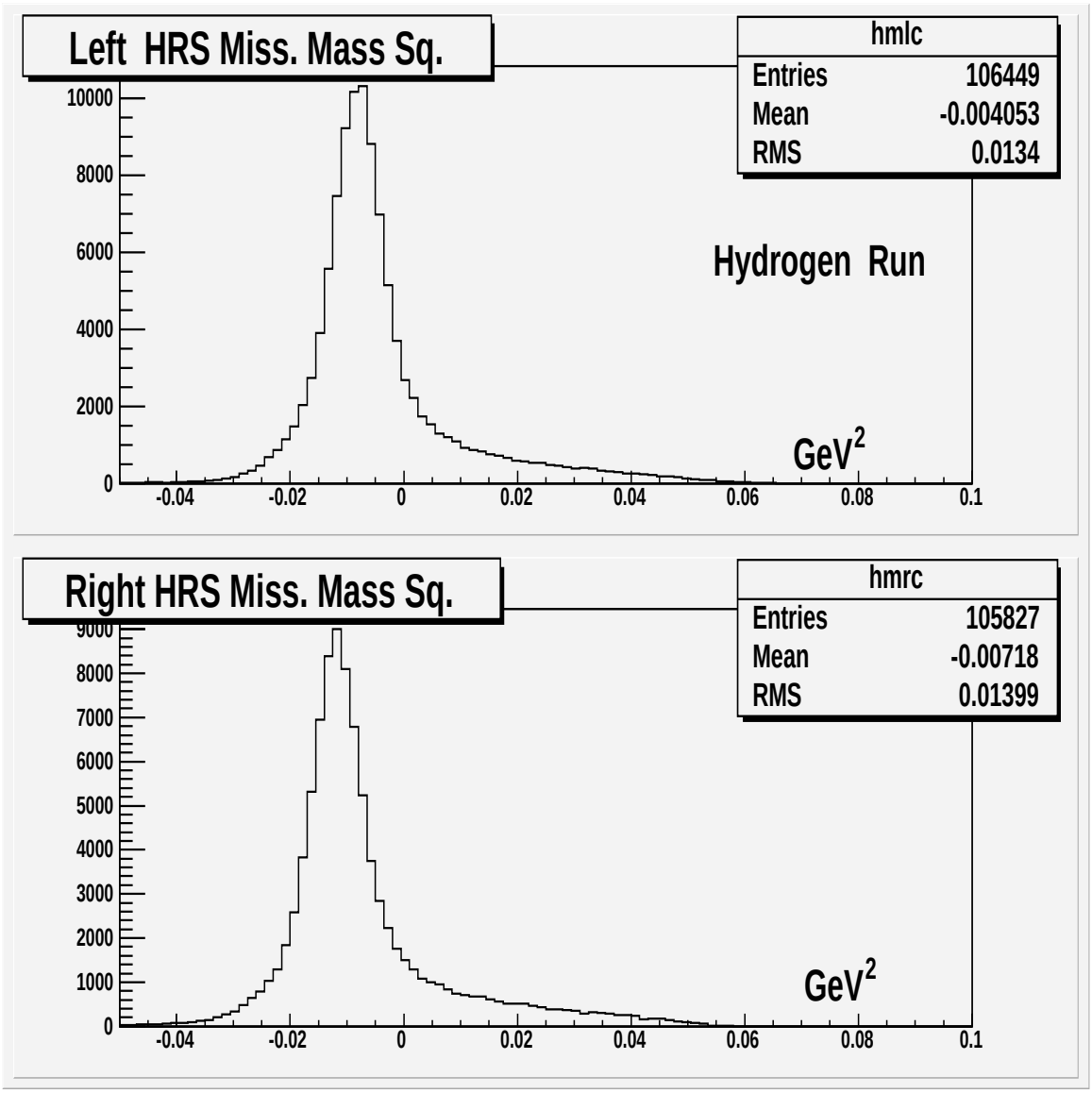

FIG. 9: Missing Mass distribution for the 2004 HAPPEX Hydrogen run. The shift away from zero indicates residual energy systematics of order a few MeV.